International Journal of Thermophysics, Vol. 19, No. 2, 1998

Nonequilibrium Molecular Dynamics Simulation of the Rheology of Linear and Branched Alkanes[1]

S. T. Cui,[2-4] P. T. Cummings,[2, 3] H. D. Cochran,[3, 2] J. D. Moore,[2, 3] and S. A. Gupta[2,3]

Liquid alkanes in the molecular weight range of C_{20}–C_{40} are the main constituents of lubricant basestocks, and their rheological properties are therefore of great concern in industrial lubricant applications. Using massively parallel supercomputers and an efficient parallel algorithm, we have carried out systematic studies of the rheological properties of a variety of model liquid alkanes ranging from linear to singly branched and multiply branched alkanes. We aim to elucidate the relationship between the molecular architecture and the viscous behavior. Nonequilibrium molecular dynamics simulations have been carried out for *n*-decane ($C_{10}H_{22}$), *n*-hexadecane ($C_{16}H_{34}$), *n*-tetracosane ($C_{24}H_{50}$), 10-*n*-hexylnonadecane ($C_{25}H_{52}$), and squalane (2, 6, 10, 15, 19, 23-hexamethyltetracosane, $C_{30}H_{62}$). At a high strain rate, the viscosity shows a power-law shear thinning behavior over several orders of magnitude in strain rate, with exponents ranging from -0.33 to -0.59. This power-law shear thinning is shown to be closely related to the ordering of the molecules. The molecular architecture is shown to have a significant influence on the power-law exponent. At a low strain rate, the viscosity behavior changes to a Newtonian plateau, whose accurate determination has been elusive in previous studies. The molecular order in this regime is essentially that of the equilibrium system, a signature of the linear response. The Newtonian plateau is verified by independent equilibrium molecular dynamics simulations using the Green–Kubo method. The reliable determination of the Newtonian viscosity from nonequilibrium molecular simulation permits us to calculate the viscosity index for squalane. The viscosity index is a widely used property to characterize the

[1] Paper presented at the Thirteenth Symposium on Thermophysical Properties, June 22–27, 1997, Boulder, Colorado, U.S.A.

[2] Department of Chemical Engineering, University of Tennessee, Knoxville, Tennessee 37996-2200, U.S.A.

[3] Chemical Technology Division, Oak Ridge National Laboratory, Oak Ridge, Tennessee 37831-6268, U.S.A.

[4] To whom correspondence should be addressed.

0195-928X/98/0300-0449$15.00/0

lubricant's temperature performance, and our studies represent the first approach toward its determination by molecular simulation.

KEY WORDS: alkanes; nonequilibrium molecular dynamics; order tensor; rheology; shear thinning; viscosity; viscosity index.

1. INTRODUCTION

The rheological properties of liquid alkanes of intermediate molecular sizes (C_{20}–C_{40}) are among the most important properties in lubricant performance. However, a thorough, realistic study of these systems by molecular simulations has previously been limited by the high computational cost. With the advent of the massively parallel supercomputers, it is now possible to carry out systematic studies of these systems with the objective of identifying the most important factors affecting the rheology. This can provide significant insight and guidance to the design of synthetic lubricants with desired properties.

Computer simulation has contributed considerably to our current understanding of the structural and rheological properties of liquid alkanes. Nonequilibrium molecular dynamics simulations (NEMD) [1], in particular, have played a major role in characterizing the properties of the alkane chains under the conditions of planar Couette shear flow. Early NEMD simulations have been limited to either relatively short chains or very short-ranged intermolecular potentials. Simulations for eicosane ($C_{20}H_{42}$) by Morris et al. [2], for example, used a WCA (Weeks, Chandler, and Andersen) potential for the intermolecular site–site interaction. Simulations carried out for *n*-hexadecane ($C_{16}H_{34}$) by Berker et al. [3] used a more realistic potential with a longer cutoff so that attractive interactions were included. In the last few years, works have appeared which focus on the rheological property of relatively longer alkanes and alkanes with more complex molecular architecture [4, 5]. In addition, early NEMD simulations were carried out at relatively high strain rates because of high computational expense at low strain rates. As a result, the Newtonian plateau region was not reached and there exist substantial uncertainties as to how to extrapolate the NEMD results to obtain reliably the Newtonian viscosity, one of the most important quantities of interest in industrial applications.

A recent model proposed by Siepmann et al. [6] accurately predicted the phase envelope of the linear alkanes from C_6 to C_{48}. The model was subsequently used by Mundy et al. [7] and Cui et al. [8] to predict quantitatively the viscosity of normal decane under a liquid state condition similar to those in the phase envelope calculations (high temperature,

moderately high density). The model was assessed by Mondello and Grest [9] for a number of equilibrium properties under near-ambient temperature conditions. The diffusion coefficient was found to be in reasonable agreement with experimental results for decane but less so for tetracosane. The same model was also used by Stevens et al. [10] and Gupta et al. [11] in their boundary layer lubrication studies. It is thus of interest from both a practical and a fundamental point of view to extend the rheological studies of decane to the ambient temperature conditions and to longer and more complex alkanes at liquid conditions.

We have recently implemented a multiple time step algorithm to perform molecular simulations for chain molecules under planar Couette flow on massively parallel supercomputers, particularly the Intel Paragon [8, 12]. This allows us systematically to study the rheological properties of liquid alkanes with molecular sizes of industrial interest. In the following sections, we describe the result of our NEMD simulations on linear and branched alkanes in the range of C_{10}–C_{30}.

2. EQUATIONS OF MOTION AND THEORY

The equations of motion used for liquid alkanes under planar Couette flow are the SLLOD [1] equations with Nosé dynamics [8],

$$\begin{aligned} \dot{\vec{r}}_{ia} &= \frac{\vec{p}_{ia}}{m_{ia}} + \gamma y_{ia}\hat{x} \\ \dot{\vec{p}}_{ia} &= \vec{F}_{ia} - \gamma p_{y,ia}\hat{x} - \zeta \vec{p}_{ia} \\ \dot{\zeta} &= \frac{p_\zeta}{Q} \\ \dot{p}_\zeta &= F_\zeta \end{aligned} \tag{1}$$

where $\vec{r}_{ia}$ and $\vec{p}_{ia}$ are the coordinates and momentum of atom a in molecule i, y_{ia} and $p_{y,ia}$ are its y components, m_{ia} is the mass, and $\hat{x}$ is a unit vector in the x direction. The quantities ζ, p_ζ, and Q are the variables related to the Nosé thermostat, $F_\zeta = \sum_{i,a}(p_{ia}^2/m_{ia}) - 3Nk_BT$, $Q = 3Nk_BT\tau^2$, τ is the Nosé thermostat time constant, and N is the total number of atoms in the system.

In a NEMD calculation, the strain rate-dependent viscosity η is determined from the constitutive relation

$$\eta = -\frac{\langle P_{xy}\rangle + \langle P_{yx}\rangle}{2\gamma} \tag{2}$$

where $\langle P_{xy} \rangle$ and $\langle P_{yx} \rangle$ are the averages of the xy and yx components of the pressure tensor $\mathbf{P}$ and γ is the strain rate characterizing the shear field. We have chosen the x direction to be the flow direction and the y direction to be the flow gradient direction, so that $\gamma = \partial u_x / \partial y$, where u_x is the streaming velocity in the x direction.

Note that a distinction should be made of whether the atomic or molecular tensor is used in Eq. (2). A number of publications have discussed the subject of the atomic and molecular pressure tensor formalisms in molecular simulation. For a system at equilibrium in the absence of an external force, the equivalence between the two in calculating the transport coefficients has been analytically proven [13, 14] and numerically verified [13,15]. For a system in planar Couette flow, the equivalence between the two has been discussed by Edberg et al. [16]. In our NEMD simulation, as the streaming velocity is applied to the atomic site, the corresponding pressure tensor $\mathbf{P}$ is calculated using the atomic formalism.

$$\mathbf{P}V = \sum_{i,a} m_{ia} \vec{v}_{ia} \vec{v}_{ia} + \frac{1}{2} \underbrace{\sum_{i,a} \sum_{j,b}}_{i \neq j} (\vec{r}_{ia} - \vec{r}_{jb}) \vec{f}_{ia,jb} + \sum_{i,a} \delta \vec{r}_{ia} \vec{f}_{ia}^{(\text{intra})} \tag{3}$$

where indices i and j refer to molecules i and j; indices a and b refer to interactions sites a and b in molecules i and j, respectively; $\vec{f}_{ia,jb}$ is the interaction force between site a on molecule i and site b on molecule j; $\delta \vec{r}_{ia}$ is the position vector of site a on molecule i relative to the center of mass of molecule i; $\vec{f}_{ia}^{(\text{intra})}$ is the total intramolecular force on site a on molecule i; and m_{ia}, $\vec{r}_{ia}$, and $\vec{v}_{ia}$ are the mass, position, and velocity, respectively, of site a on molecule i. Note that since the total intramolecular force sums to zero for a given molecule, the last term in Eq. (3) does not depend on the choice of origin in the determination of $\delta \vec{r}_{ia}$, so this can be conveniently chosen to be the center of mass of the molecule.

In our equilibrium molecular dynamics (EMD) simulation, the pressure tensor is calculated using the molecular formalism,

$$\mathbf{P}^{(m)} V = \sum_{i} m_i \vec{v}_i \vec{v}_i + \frac{1}{2} \underbrace{\sum_{i} \sum_{j}}_{i \neq j} (\vec{r}_i - \vec{r}_j) \vec{F}_{ij} \tag{4}$$

where $\vec{F}_{ij}$ is the force between the centers of mass of molecules i and j, and m_i, $\vec{r}_i$, and $\vec{v}_i$ are the mass, position, and velocity, respectively, of molecule i. The viscosity is calculated according to the Green–Kubo formula, as given in Ref. 1.

$$\eta = \frac{V}{k_B T} \int_0^\infty dt \langle P_{xy}^{(m)}(t) \, P_{xy}^{(m)}(0) \rangle \tag{5}$$

In this equation, $\langle P_{xy}^{(m}(t\, P_{xy}^{(m)}(0)\rangle$ is the correlation function of the xy component of the symmetric part of the molecular pressure tensor.

3. RESULTS AND DISCUSSION

The systems and the state conditions we have studied are tabulated in Table I. These include linear C_{10} (*n*-decane), C_{16} (*n*-hexadecane), and C_{24} (*n*-tetracosane); long but singly branched C_{25} (10-*n*-hexylnonadecane); and multiply short-branched C_{30} (squalane). In Fig. 1, the viscosity of the liquid alkanes of various molecular lengths and architectures is plotted vs the applied strain rate. In general, all systems exhibit similar overall characteristics under the planar Couette shear flow. At a low strain rate, the viscosity of the alkanes shows a plateau region. As the strain exceeds a certain value, dependent on the molecular architecture and the state condition of the liquid, the viscosity begins to decrease with the increasing strain rate (shear thinning). The viscosity values in the shear thinning region are strongly influenced by the molecular architecture. For the linear alkanes, the viscosities at high strain rates differ very slightly. When branches are added (e.g., for 10-*n*-hexylnonadecane, which has one hexyl branch, and squalane, which has six methyl side groups), the viscosity at high strain rates increases significantly. The slope of the shear thinning region follows a power law, with the exponent closely related to the chain length for linear alkanes and the backbone length and molecular architecture for the branched alkanes. The exponents were determined to be -0.33 (*n*-decane), -0.39 (*n*-hexadecane), -0.41 (*n*-tetracosane), -0.48 (10-*n*-hexylnonadecane), -0.45 (squalane; $T=372$ K), and -0.59 (squalane; $T=311$ K). It is worth noting that similar behavior of the viscosity vs strain rate is observed for polymeric liquids, with the exponent between

Table I. State Points of the Simulations.

Alkane	T(K)	Density (g · cm^{-3})[a]
n-decane	298	0.7247[b]
n-hexadecane	323	0.753
n-tetracosane	333	0.773
10-*n*-hexylnonadecane	333	0.7762[c]
Squalane	311	0.7979
	372	0.7592

[a] Densities are from Ref. 23 unless noted otherwise.

[b] From Ref. 24.

[c] From Ref. 25; the density was obtained by extrapolation from the data for 8-*n*-hexylpentadecane and 9-*n*-hexylheptadecane listed in Ref. 23.

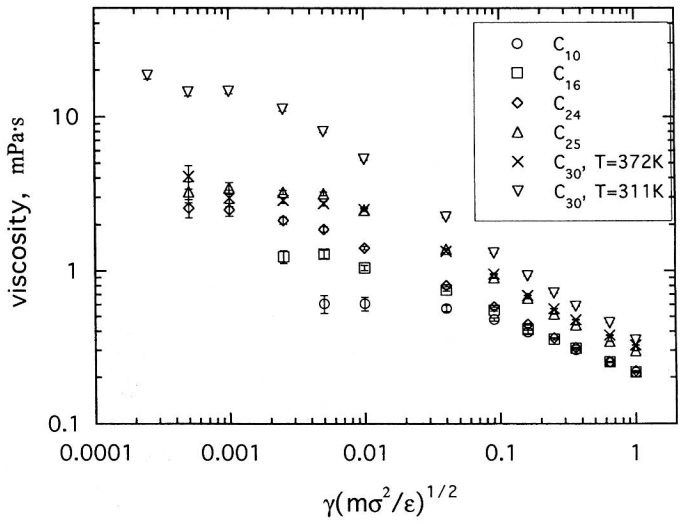

Fig. 1. The viscosity of linear and branched alkanes vs the strain rate. The strain rate is in reduced units, where m = amu, $\varepsilon = 47$ K, and $\sigma = 3.93$Å are the mass, Lennard–Jones energy, and length parameters of a CH_2 group, respectively. Circles, *n*-decane; squares, *n*-hexadecane; diamonds, *n*-tetracosane; triangles, 10-*n*-hexylnonadecane; crosses, squalane ($T = 372$ K); inverted triangles, squalane ($T = 311$ K).

about -0.4 and -0.9 [17]. This suggests that although the alkanes chains (or the backbone for branched alkanes) studied here are very short in comparison to polymeric molecules, they nevertheless exhibit some of the generality of the chain systems in response to the shear flow.

The determination of the Newtonian viscosity from the NEMD simulation has been somewhat arbitrary in earlier studies of alkane liquids, because of the very long runs required to determine the low-strain rate shear viscosity with sufficient accuracy and, hence, reliably extrapolate the zero-strain rate viscosity. This is in contrast to simple atomic systems, where an extrapolation using the analytical expression $\eta = \eta_0 - \alpha\gamma^{1/2}$ results in an error which can be reasonably neglected, and the strain rate-dependent viscosity in the whole shear thinning region can be used to determine the zero-strain rate viscosity. For alkanes, since the strain rate-dependent viscosity follows a power-law behavior and the exponent is negative, the strain rate-dependent viscosity in the shear thinning region cannot be used for the extrapolation, and accurate values of viscosity in the Newtonian region must be obtained for the extrapolation. We carried out long simulations for the calculation of the viscosity of alkanes at a low strain rate for the systems studied in this work. For the two or three data points at the

lowest strain rates in the viscosity-vs-strain rate plot, we observed the plateau behavior of the viscosity as shown in Fig. 1. These plateau values can be used to determine the Newtonian viscosity of the alkanes. To verify independently the Newtonian viscosity obtained from the plateau value of the NEMD calculation, we also carried out equilibrium calculations using the Green–Kubo method to determine the zero-strain rate viscosity for *n*-decane and *n*-hexadecane at the same temperature and density as the NEMD calculation. For *n*-decane, we find $\eta = 0.61 \pm 0.08$ mPa · s) from NEMD and $\eta = 0.64 \pm 0.05$ mPa · s from Green–Kubo. For *n*-hexadecane, we obtain $\eta = 1.24 \pm 0.12$ mPa · s from NEMD and $\eta = 1.17 \pm 0.17$ mPa · s from the Green–Kubo method. Independent equilibrium calculations by Mondello and Grest [18] give $\eta = 1.11 \pm 0.10$ mPa · s for *n*-hexadecane, which is in excellent agreement with our NEMD and Green–Kubo calculations. These results suggest that NEMD can be used to determine the Newtonian viscosity reliably for alkane liquids (at least for the short alkanes) and that the proper extrapolation should be from the constant plateau value at low strain rates in the Newtonian region of the viscosity. We also observe that, since at a high strain rate the viscosity of linear alkanes varies only slightly with chain length, the value of the Newtonian viscosity is essentially determined by the range of the shear thinning region, which is correlated with the rotational relaxation time (see below). For branched alkanes, the Newtonian viscosity depends on both the rotational relaxation and the molecular architecture.

The transition from the Newtonian region to the shear thinning region indicates some type of structural order in the system under shear flow. When the shear field exceeds the inverse of the relaxation time of the liquid, the system cannot respond fast enough to the deformation due to the flow field so that some degree of ordering begins to appear, resulting in a reduced viscosity. For liquid alkanes, the most relevant structural order is the orientational order of the alkane molecules. The time scale of such ordering is measured by the longest rotational relaxation time. In our previous work [4] and work by Mondello and Grest [9], the rotational relaxation times have been determined for *n*-decane, *n*-hexadecane, *n*-tetracosane, and squalane. Under the state conditions reported in this work, the relaxation times are $\tau = 58$ ps for *n*-decane, $\tau = 188$ ps for *n*-hexadecane, $\tau = 531$ ps for *n*-tetracosane, and $\tau = 2.85$ ns at $T = 311$ K and $\tau = 0.464$ ns at $T = 372$ K for squalane. The inverse of the rotational relaxation time corresponds to the reduced strain rate: $\gamma^* = 0.041$ for *n*-decane, $\gamma^* = 0.0125$ for *n*-hexadecane, $\gamma^* = 0.0044$ for *n*-tetracosane, and $\gamma^* = 0.00082$ at $T = 311$ K and $\gamma^* = 0.00506$ at $T = 372$ K for squalane. These values correlate reasonably well with the transition from the Newtonian region to the shear thinning region in Fig. 1. It should be noted that, in general, the

transition is not a sharp one but a gradual one, as no phase change is expected.

Accompanying the shear thinning behavior is the alignment of the molecules with the flow direction. One measure of such structural order is the order tensor, which is defined as [19]

$$\boldsymbol{S}=\frac{3}{2}\left\langle\frac{1}{N}\sum_{i=1}^{N}\left(\boldsymbol{e}_i\boldsymbol{e}_i-\frac{1}{3}\boldsymbol{I}\right)\right\rangle \tag{6}$$

where $\boldsymbol{e}_i$ is the unit vector along the end-to-end direction of a molecule i (for branched alkanes, the end-to-end vector is defined along some prescribed direction, or the backbone direction, as is the case for squalane), $\boldsymbol{I}$ is a unit second-rank tensor, and the summation is over all N molecules in the system. The angle braces indicate an ensemble average. The eigenvector corresponding to the largest eigenvalue of the order tensor gives the preferential orientation of the end-to-end vector of the alkane molecules relative to the flow field. Our results on the aligment angles for n-decane, n-hexadecane, n-tetracosane, and squalane (at $T=372$ K) are plotted in Fig. 2. At a very low strain rate, the alignment angles tend to 45°, as expected from the prediction of the birefringence [20] for a linear regime. At a very high strain rate, the alkane molecules are aligned with a preferred angle which depends on the length of the molecule (or the backbone). As the chain length increases, the alignment angle at a high strain decreases,

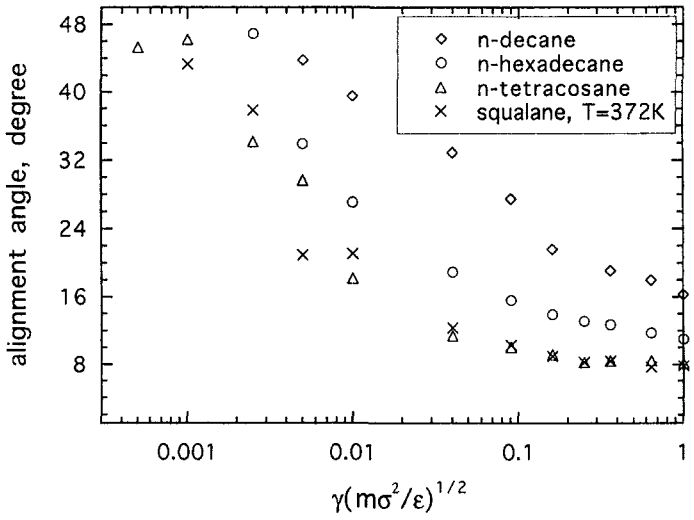

Fig. 2. The alignment angle with the flow field of the end-to-end vector for n-decane, n-hexadecane, and n-tetracosane and of the backbone for squalane.

suggesting that the longer molecules must be better aligned with the flow field to dissipate the viscous force among themselves. The transition of the fluid from the essentially isotropic structure to the highly orientationally ordered structure is fairly sharp. This transition becomes more obvious for longer molecules. For *n*-hexadecane, for example, the alignment angle decreases from 45° to about 20° when the strain rate increases by only one decade. Further increase in the strain rate decreases the alignment angle only slightly, i.e., the alignment of molecules appears to saturate at high strain rates. A comparison of Figs. 1 and 2 suggests that the sharp decrease in the alignment angle is correlated with the transition of the viscosity vs strain rate from the Newtonian region to the shear thinning region, while the essentially saturated region is correlated with the power-law shear thinning region of the viscosity-vs-strain rate plot. We note further that *n*-tetracosane and squalane ($T = 372$ K) tend essentially to the same alignment angle at high strain rates, while the corresponding viscosity for squalane is much higher than for *n*-tetracosane in this region. This suggests that the addition of branches has a significant effect on the viscosity of the fluid.

In industrial applications, it is important that a lubricant have an essentially constant viscosity over a range of temperatures so that its performance is not degraded by changing temperature conditions. This temperature behavior of lubricants is characterized by the viscosity index [21, 22]. Different viscosity index definitions have been used over time as lubricant performance has been improved. The currently accepted definition of the viscosity index (VI) is given by

$$\mathrm{VI} = 3.63[60 - \exp(n)] \tag{7}$$

where n is given by

$$n = \frac{\log \nu_1 - \log k}{\log \nu_2} \tag{8}$$

where ν_1 is the kinematic viscosity at temperature $T = 311$ K, ν_2 is the kinematic viscosity at temperature $T = 372$ K, and $k = 2.714$ is a function of the temperature range alone and is independent of the nature of the lubricant. The interested reader is referred to the original literature [21, 22] for detailed information and the significance of the constant introduced in Eqs. (7) and (8). Using the zero-strain rate viscosity determined for squalane at $T = 311$ and 372 K, Eqs. (7) and (8) yield a viscosity index value of 119 for squalane, which is in excellent agreement with the experimental value of 123 [23].

4. CONCLUSIONS

In this paper, we have presented NEMD simulations of the viscosity–strain rate behavior for a number of linear and branched liquid alkanes of applicational importance in industry. We found that the addition of branches can significantly increase the viscosity of the liquid. The transition of the viscosity from Newtonian to shear thinning is correlated with a sharp decrease in the preferred alignment angle of alkane molecules with the flow field. The strain rate at which the transition takes place is correlated with the rotational relaxation time of alkane molecules in the system. The power-law shear thinning is correlated with a near-saturation of the alignment of the molecules with the flow field. From the Newtonian viscosities determined by the NEMD simulations, we have calculated the viscosity index for squalane, which is in excellent agreement with experiment.

ACKNOWLEDGMENTS

This work was sponsored by the Laboratory Directed Research and Development Program of ORNL. The work of H.D.C. was supported by the Division of Chemical Sciences of the U.S. Department of Energy. The authors acknowledge the use of the Intel Paragon supercomputers at the Center for Computational Sciences at ORNL, funded by the DOE's Mathematical, Information, and Computational Sciences Division. ORNL is managed by Lockheed Martin Energy Research Corp. for the DOE under Contract DE-AC05-96OR22464.

REFERENCES

1. D. J. Evans and D. P. Moriss, *Statistical Mechanics of Nonequilibrium Liquids* (Academic Press, London, 1990), Chap. 6.
2. G. P. Morris, P. T. Daivis, and D. J. Evans, *J. Chem. Phys.* **94**:7420 (1991).
3. A. Berker, S. Chinoweth, U. C. Klomp, and Y. Michopoulos, *J. Chem. Soc. Faraday Trans.* **88**:1719 (1992).
4. S. T. Cui, S. A. Gupta, P. T. Cummings, and H. D. Cochran, *J. Chem. Phys.* **105**:1214 (1996).
5. J. D. Moore, S. T. Cui, P. T. Cummings, and H. D. Cochran, *AICHE J.* **43**:3260 (1997).
6. J. I. Siepmann, S. Karaborni, and B. Smit, *Nature* **365**:330 (1993).
7. C. J. Mundy, J. I. Siepmann, and M. L. Klein, *J. Chem. Phys.* **102**:3376 (1995).
8. S. T. Cui, P. T. Cummings, and H. D. Cochran, *J. Chem. Phys.* **104**:255 (1996).
9. M. Mondello and G. S. Grest, *J. Chem. Phys.* **103**:7156 (1995).
10. M. J. Stevens, M. Mondello, G. S. Grest, S. T. Cui, H. D. Cochran, and P. T. Cummings, *J. Chem. Phys.* **106**:7303 (1997).

11. S. A. Gupta, P. T. Cummings, and H. D. Cochran, *J. Chem. Phys.* **107**:10316 (1997); op. cit. 10327; op. cit. 10335.
12. H. D. Cochran, P. T. Cummings, S. T. Cui, S. A. Gupta, R. K. Bhupathiraju, and P. F. LaCascio, *Comp. Math. Appl.* **35**:73 (1998).
13. G. Maréchal and J. P. Ryckaert, *Chem. Phys. Lett.* **101**:548 (1983).
14. M. P. Allen, *Mol. Phys.* **52**:705 (1984).
15. S. T. Cui, P. T. Cummings, and H. D. Cochran, *Mol. Phys.* **88**:1653 (1996).
16. R. Edberg, G. P. Morris, and D. J. Evans, *J. Chem. Phys.* **86**:4555 (1987).
17. H. A. Barnes, J. F. Hutton, and K. Walters, *An Introduction to Rheology* (Elsevier, Amsterdam, 1989).
18. M. Mondello and G. S. Grest, *J. Chem. Phys.* **106**:9329 (1997).
19. S. Chandrasekhar, *Liquid Crystals*, 2nd ed. (Cambridge University Press, Cambridge, 1992); P. G. de Gennes and J. Prost, *The Physics of Liquid Crystals*, 2nd ed. (Clarendon Press, Oxford, 1993).
20. J. C. Maxwell, *Proc. R. Soc. London Ser. A* **22**:151 (1873).
21. E. W. Dean and G. H. B. Davis, *Chem. Met. Eng.* **36**:618 (1929).
22. Hardimann and A. H. Nissan, *J. Inst. Petrel.* **31**:255 (1945).
23. API, *API 42, Properties of Hydrocarbons of High Molecular Weight* (American Petroleum Institute, Research Project 42, Washington, D.C., 1966).
24. M. Gehrig and H. Lentz, *J. Chem. Thermodyn.* **15**:1159 (1983).
25. Personal communication with M. Mondello (1996).